ORIGINAL PAPER

Prolonged persulfate activation by UV irradiation of green rust for the degradation of organic pollutants

Yiqun Chen[1,2] · Shuxian Gao[1] · Zizheng Liu[1,2] · Senlin Shao[1,2] · Weizhao Yin[3] · Zheng Fang[1,2] · Li-Zhi Huang[1,2]

Abstract

Metal-activated persulfate is an efficient reagent for the oxidative degradation of organic contaminants. However, homogenous catalytic activation of persulfate has the drawbacks of narrow pH range and metal ion contamination. Here, we designed a heterogeneous system for persulfate activation by green rust irradiated with ultraviolet light-emitting diode for the removal of organic pollutants. Generated radicals were identified through radical quenching experiments. Results show that benzoic acid can be degraded. Although structural Fe^{II} in green rust can activate persulfate, the rapid oxidation of Fe^{II}–Fe^{III} by persulfate quickly ceases further persulfate activation in the absence of UV irradiation. Here, UV irradiation reduces the generated Fe^{III} on the surface of green rust to Fe^{II} for prolonged persulfate activation. The highest benzoic acid degradation was obtained with 1.0 mM persulfate and 0.5 mM green rust, expressed as Fe^{II} concentration. $HO^{.}$ is the main oxidative species responsible for benzoic acid degradation.

Keywords Green rust · Persulfate · UV-LED · Sulfate radical · Hydroxyl radical · Benzoic acid

Introduction

Green rusts are a type of mixed Fe(III) and Fe(II) minerals with a unique layered structure, which consist of positively charged iron(II)–iron(III) hydroxide layers which is compensated by anions, i.e., Cl^-, SO_4^{2-}, and CO_3^{2-}, situated between layers (Simon et al. 2003). Green rusts are intermediate phases formed by partial oxidation of Fe(II) minerals or partial reduction of Fe(III) (hydr)oxides in the environment (O'Loughlin et al. 2007). Green rust has a strong reducing strength due to the fact that the structure iron(II) in green rusts hold high electron-donating potential, and the charge hoping within iron(II)–iron(III) hydroxide layers is very fast (Wander et al. 2007). Green rusts are known to reduce various forms of reducible pollutants (Erbs et al. 1999; Lee and Batchelor 2002; Mitsunobu et al. 2008), but the use of green rust in advance oxidation process to remove organic pollutants has been rarely studied. Few researchers have used green rust in Fenton-like process for degradation of organic pollutants including phenol and azo dyes (Hanna et al. 2010; Kone et al. 2009; Lin et al. 2014; Matta et al. 2008). The surface-normalized pseudo-first-order rate constants for phenol degradation are in the range from 0.4×10^{-4} L m^{-2} s^{-1} to 13×10^{-4} L m^{-2} s^{-1}, and significant total organic carbon removal (87%) was observed for methyl red degradation (Hanna et al. 2010; Kone et al. 2009).

Activated persulfate oxidation has recently been developed as an alternative advanced oxidation process through the generation of sulfate radicals (SO_4^-) (Yu et al. 2016; Zhang et al. 2018; Zhou et al. 2017). Compared to $HO^{.}$ ($E° = 1.8$–2.7 V), SO_4^- is believed to have comparable redox potential ($E° = 2.5$–3.1 V), but better selectivity and stability via electron transfer with organic compounds (Luo et al. 2017, 2018). Persulfate activation by iron-bearing minerals has been widely investigated and used in water remediation (Liu et al. 2014), but persulfate activation by green rust is completely ignored.

✉ Senlin Shao
   shaosenlin@whu.edu.cn

✉ Li-Zhi Huang
   lizhihuang@whu.edu.cn

1   School of Civil Engineering, Wuhan University, Wuhan 430072, People's Republic of China

2   Engineering Research Center of Urban Disasters Prevention and Fire Rescue Technology of Hubei Province, Wuhan University, Wuhan 430072, People's Republic of China

3   School of Environment, Jinan University, Guangzhou 510632, People's Republic of China

A common limitation for Fe/persulfate process is the precipitation of ferric hydroxide and slow transformation from Fe^{III} to Fe^{II}. To overcome this drawback, UV light has been generally adopted since it promotes Fe(III)/Fe(II) redox cycle (Wang et al. 2018a, b). Although the photochemistry of green rust is scarcely studied, the photoreduction of Fe(III) to Fe(II) in iron-bearing minerals-activated persulfate system is widely reported (Avetta et al. 2015). Similar phenomenon may occur, and the restoration of green rust reactivity via UV irradiation is expected.

In this work, we investigated the activation of persulfate by green rust and explored the synergistic effect of UV-LED irradiation. Benzoic acid was used as a model compound to evaluate the performance and mechanism of this novel system.

Experimental

Chemicals and materials

Glycine was obtained from Sigma-Aldrich Co. (St. Louis, MO, USA). Other chemicals were all analytical grade and purchased from Sinopharm Chemical Reagent Co., Ltd. (Shanghai, China). Sulfate-interlayered green rust was synthesized via co-precipitation of Fe^{II} and Fe^{III} in the presence of glycine at pH 8.0, as previously described (Yin et al. 2017). Ultrapure water (18.2 MΩ cm) was used throughout the experiments.

UV-LED-assisted activation of persulfate by green rust

A commercial UV-LED light (78 UU, 7 W) which radiates at 365 nm was purchased from Zigu Limited, Zhongshan, People's Republic of China. The UV-LED light system was placed on top of a 500-mL reactor which was magnetic stirred at 1000 rpm. The distance between the UV-LED light and the surface of the reaction solution is 3 cm with a radiation intensity of 200 mW m^{-2}. The reaction temperature was controlled at 22 °C. All the O_2-free solutions were prepared by Ar bubbling with a flow of 30 mL min^{-1} for sufficient time (1–3 h). All experiments were carried out in glovebox (Mikrouna, Inc. P.R.C.) filled with Ar gas to maintain O_2-free conditions during reactions. Green rust was firstly dispersed into 500 mL O_2-free benzoic acid solution (20 μM), and the mixture was stirred for 15 min to achieve the adsorption/desorption equilibrium between green rust and benzoic acid. Subsequently, freshly prepared persulfate stock solution (1.0 M) was added into the solution. Persulfate activation by green rust was carried out at the same conditions but without UV irradiation. The pH of the reaction in all the experiments was adjusted to seven using H_2SO_4

or NaOH. Only neutral pH is used in this work, because green rust is only stable around pH 7.0. Low pH will lead to dissolution of green rust in solution, and high pH will lead to the transformation of green rust to other iron oxides such as magnetite. Once the photodegradation was initiated, 1 mL sample was collected from the reaction suspensions at given time intervals from 2 to 60 min, immediately quenched by excess methanol, filtered by 0.22-μm membrane filter and analyzed by high-performance liquid chromatography (HPLC).

Analytical methods

Benzoic acid was analyzed with HPLC (1220 Infinity II LC System, Agilent), equipped with an Eclipse XDB–C18 column (5 μm, 250 mm × 4.6 mm). The eluent consisted of 10 mM phosphoric acid solution in methanol mixture (1/1, v/v). The injection volume was 100 μL, and the flow rate was 1.0 mL min^{-1}. UV/Vis detection was carried out at a wavelength of 228 nm. The concentration of Fe^{II} in green rust was determined in glovebox using a modified 1,10-phenanthroline method (Huang et al. 2013).

Results and discussion

Benzoic acid degradation in UV/green rust/persulfate process

Adsorption of benzoic acid onto green rust is negligible as its concentration in bulk solution is constant in a stirred green rust suspension for 60 min (Fig. 1a). Applying UV irradiation does not benefit the benzoic acid degradation by green rust, demonstrating that green rust surface cannot be activated by UV to produce reactive species. Besides, no degradation of benzoic acid occurred in the presence of either UV (data not shown) or persulfate alone. In contrast, UV/persulfate process degraded 46.0% of benzoic acid, which can be ascribed to the produced $SO_4^{\cdot-}$ and $HO^\cdot$ via Eqs. (1) and (2).

$$S_2O_8^{2-} + h\nu \rightarrow 2SO_4^{\cdot-} \tag{1}$$

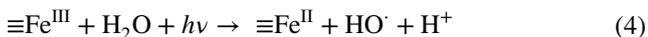$$SO_4^{\cdot-} + OH^- \rightarrow HO^\cdot + SO_4^{2-} \tag{2}$$
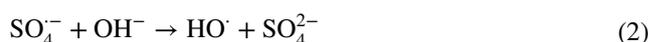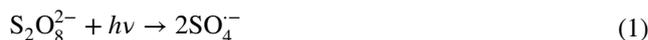
Moreover, up to 32% of benzoic acid was removed by green rust/persulfate process in the first 10 min, indicating that persulfate can also be activated by the strong reductant green rust as proposed in Eq. (3). However, no further degradation of benzoic acid was observed properly due to the full oxidation of Fe^{II} sites in green rust. It should be noted that benzoic acid was almost completely degraded when combining UV with green rust/persulfate process. The results can
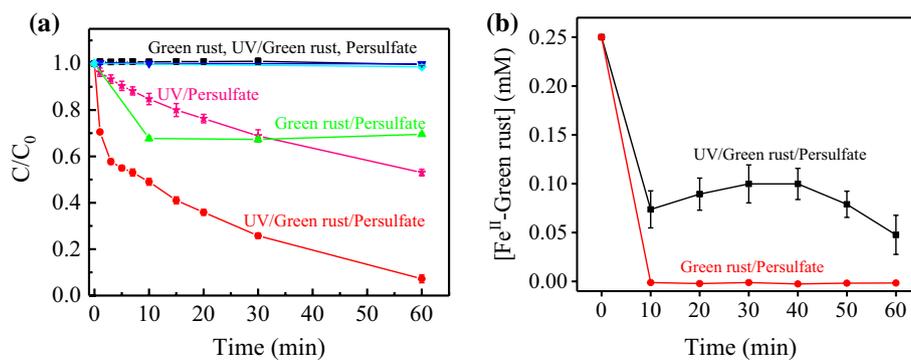
Fig. 1 a Degradation of benzoic acid in different processes, b variation of Fe^{II}-green rust during reaction course in UV/green rust/persulfate and green rust/persulfate process. Experimental conditions [benzoic acid]$_0$ = 20 μM, [persulfate]$_0$ = 1 mM, [Fe^{II}-green rust]$_0$ = 0.25 mM, pH$_0$ = 7. The high benzoic acid degradation efficiency in UV/green rust/persulfate process shown in (a) may be due to the photogeneration of Fe^{II}-green rust sites after 10-min reaction shown in (b)

be explained by the reduction of Fe^{III} to Fe^{II} driven by UV irradiation (Eq. 4) (Dai et al. 2018), resulting in a continuous activation of persulfate.

$$\equiv Fe^{II} + S_2O_8^{2-} \rightarrow \ \equiv Fe^{III} + SO_4^{\cdot-} + SO_4^{2-} \tag{3}$$

$$\equiv Fe^{III} + H_2O + h\nu \rightarrow \ \equiv Fe^{II} + HO^{\cdot} + H^+ \tag{4}$$

To further confirm this hypothesis, Fe^{II}-green rust was monitored during the reaction. As expected, Fe^{II}-green rust was fully oxidized by persulfate in the first 10 min (Fig. 1b), which is in accordance with the fast benzoic acid degradation at the start of green rust/persulfate process (Fig. 1a). After a similar quick-drop stage in the first 10 min, the concentration of Fe^{II}-green rust increased in the presence of UV irradiation due to photoreduction of Fe^{III} sites (Eq. 4) while decreased again from 40 to 60 min. One explanation could be that green rust was transformed to lepidocrocite and magnetite which resulted in an inefficient regeneration of Fe^{II} sites.
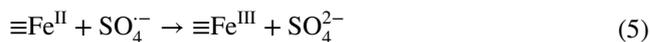
Effect of Fe^{II}-green rust loading

Figure 2 shows the benzoic acid degradation with different Fe^{II}-green rust loadings. 0.5 mM Fe^{II}-green rust loading in UV/green rust/persulfate process resulted in the highest reactivity toward benzoic acid degradation. When the concentration of active Fe^{II}-green rust sites is low, increasing the Fe^{II}-green rust loading can activate more persulfate for faster benzoic acid degradation. However, the Fe^{II}-green rust loading higher than 0.5 mM suppressed the benzoic acid degradation, which can be explained by two primary reasons: (1) The scattering of UV irradiation by excess green rust suppresses the penetration of UV irradiation, resulting in low efficiency of UV-induced persulfate activation and Fe^{II}-green rust regeneration; (2) excess Fe^{II}-green rust sites
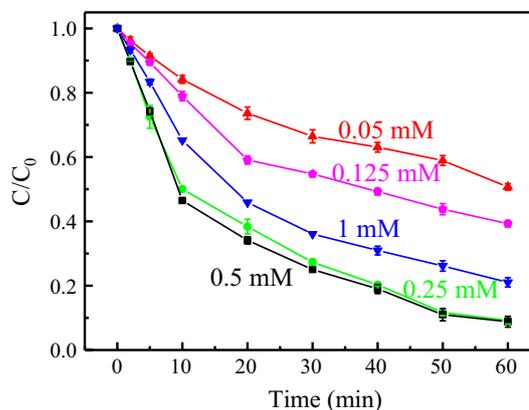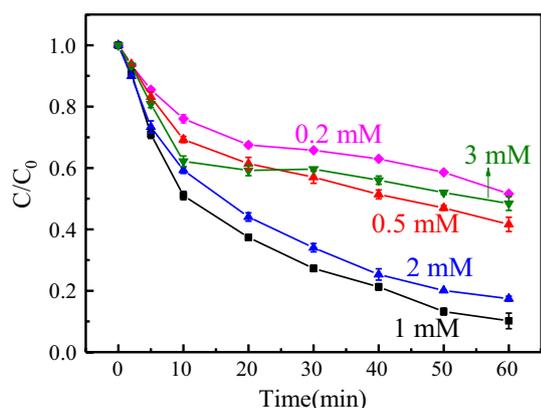

Fig. 2 Effect of Fe^{II}-green rust loading on benzoic acid degradation in UV/green rust/persulfate process. Experimental conditions [benzoic acid]$_0$ = 20 μM, [persulfate]$_0$ = 1 mM, [Fe^{II}-green rust]$_0$ = 0.05–1 mM, pH$_0$ = 7. Fe^{II}-green rust loading higher than 0.5 mM may suppress the UV penetration and compete with benzoic acid for $SO_4^{\cdot-}$ and $HO^{\cdot}$, which inhibits benzoic acid degradation

may compete with benzoic acid for $SO_4^{\cdot-}$ and $HO^{\cdot}$ (Eqs. 5, 6), which has been confirmed in Fe/persulfate process (Bu et al. 2016).

$$\equiv Fe^{II} + SO_4^{\cdot-} \rightarrow \equiv Fe^{III} + SO_4^{2-} \tag{5}$$

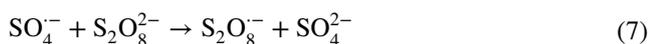$$\equiv Fe^{II} + HO^{\cdot} \rightarrow \equiv Fe^{III} + HO^- \tag{6}$$

Effect of persulfate concentration

The removal of benzoic acid in UV/green rust/persulfate process with different persulfate concentrations was investigated (Fig. 3). The benzoic acid degradation efficiency significantly increased from 48 to 90% with the persulfate concentration increasing from 0.2 to 1 mM, indicating
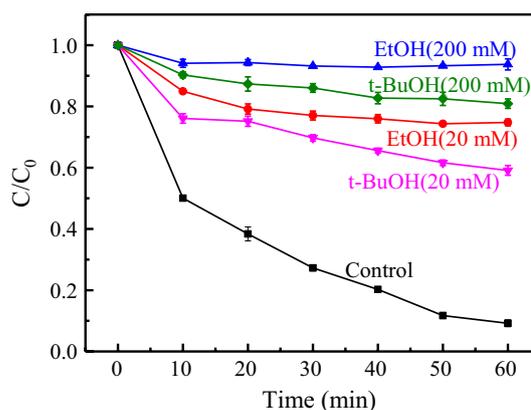
Fig. 3 Effect of persulfate concentration on benzoic acid degradation in UV/green rust/persulfate process. Experimental Conditions: [benzoic acid]$_0$ = 20 μM, [persulfate]$_0$ = 0.2–3 mM, [Fe^{II}-green rust]$_0$ = 0.25 mM, pH$_0$ = 7. Note excess persulfate may result in self-quenching of reactive radicals (SO$_4^-$ and HO$^·$), leading to a decrease in the degradation efficiency of benzoic acid

Fig. 4 Effect of EtOH and t-BuOH on benzoic acid degradation in UV/green rust/persulfate process. Experimental conditions [benzoic acid]$_0$ = 20 μM, [persulfate]$_0$ = 1 mM, [Fe^{II}-green rust]$_0$ = 0.25 mM, pH$_0$ = 7. These results demonstrate that both SO$_4^-$ and HO$^·$ are responsible for the degradation of benzoic acid in UV/green rust/persulfate system, while HO$^·$ is the dominating one

higher persulfate concentration can produce more SO$_4^{·-}$. However, further increase in persulfate concentration from 1 to 3 mM resulted in a decrease in the removal efficiency of benzoic acid from 90 to 52%. It can be explained that excess persulfate may result in self-quenching of reactive radicals (SO$_4^{·-}$ and HO$^·$) (Eqs. 7, 8) (Liu et al. 2014). Therefore, the optimal persulfate concentration for benzoic acid removal is 1 mM.

$$SO_4^{·-} + S_2O_8^{2-} \rightarrow S_2O_8^{·-} + SO_4^{2-} \tag{7}$$

$$HO^· + S_2O_8^{2-} \rightarrow S_2O_8^{·-} + HO^- \tag{8}$$

Identification of radicals

For revealing the existence of reactive radicals (SO$_4^{·-}$ and HO$^·$), ethanol (EtOH) and ter-butyl alcohol (t-BuOH) with different initial concentrations were used as scavengers in the UV/green rust/persulfate system. EtOH can effectively quench both HO$^·$ and SO$_4^{·-}$, while t-BuOH is an efficient scavenger for HO$^·$, but not for SO$_4^{·-}$ (Neta et al. 1988). As shown in Fig. 4, the removal efficiencies of benzoic acid significantly decreased to 25% and 41% when introducing 20 mM EtOH and t-BuOH into the reaction, respectively. EtOH at concentrations of 200 mM almost completely inhibited the removal of benzoic acid, whereas induction of 200 mM t-BuOH decreased the removal efficiencies of benzoic acid to 19%. These results demonstrate that both SO$_4^{·-}$ and HO$^·$ are responsible for the degradation of benzoic acid in UV/green rust/persulfate system, while HO$^·$ is the dominating one. It can be ascribed to the low concentration of Fe^{II}-green rust (Fig. 1b) after 10 min reaction, which

inhibited the generation of SO$_4^{·-}$ via Eq. (3). The results suggest that the reduction of Fe^{III}-green rust to Fe^{II}-green rust under UV irradiation along with the formation of HO$^·$ may play an important role in UV/green rust/persulfate system.

Conclusion

Green rust was used to activate persulfate under UV-LED irradiation for the first time. Experimental results show benzoic acid can be efficiently degraded in UV/green rust/persulfate process. The recycling between Fe^{II} and Fe^{III} driven by UV irradiation results in a continuous activation of persulfate, which is demonstrated by the prolonged benzoic degradation in UV/green rust/persulfate process compared to green rust/persulfate process. The optimal concentrations of Fe^{II}-green rust loading and persulfate were determined to be 0.5 mM and 1 mM, respectively. Additionally, both SO$_4^{·-}$ and HO$^·$ were evidenced to oxidize benzoic acid in UV/green rust/persulfate system, while HO$^·$ was primarily responsible for the degradation.

References

Avetta P, Pensato A, Minella M, Malandrino M, Maurino V, Minero C, Hanna K, Vione D (2015) Activation of persulfate by irradiated

magnetite: implications for the degradation of phenol under heterogeneous photo-Fenton-like conditions. Environ Sci Technol 49(2):1043–1050. https://doi.org/10.1021/es503741d

Bu LJ, Shi Z, Zhou SQ (2016) Modeling of Fe(II)-activated persulfate oxidation using atrazine as a target contaminant. Sep Purif Technol 169:59–65. https://doi.org/10.1016/j.seppur.2016.05.037

Dai HW, Xu SY, Chen JX, Miao XZ, Zhu JX (2018) Oxalate enhanced degradation of Orange II in heterogeneous UV-Fenton system catalyzed by $Fe_3O_4@\gamma$-Fe_2O_3 composite. Chemosphere 199:147–153. https://doi.org/10.1016/j.chemosphere.2018.02.016

Erbs M, Hansen HCB, Olsen CE (1999) Reductive dechlorination of carbon tetrachloride using iron(II) iron(III) hydroxide sulfate (green rust). Environ Sci Technol 33(2):307–311. https://doi.org/10.1021/es980221t

Hanna K, Kone T, Ruby C (2010) Fenton-like oxidation and mineralization of phenol using synthetic Fe(II)-Fe(III) green rusts. Environ Sci Pollut Res 17(1):124–134. https://doi.org/10.1007/s11356-009-0148-y

Huang L-Z, Ayala-Luis KB, Fang L, Dalby KN, Kasama T, Bender Koch C, Hansen HCB (2013) Oxidation of dodecanoate intercalated iron(II)–iron(III) layered double hydroxide to form 2D iron(III) (hydr)oxide layers. Eur J Inorg Chem 2013(33):5718–5727. https://doi.org/10.1002/ejic.201300735

Kone T, Hanna K, Abdelmoula M, Ruby C, Carteret C (2009) Reductive transformation and mineralization of an azo dye by hydroxysulphate green rust preceding oxidation using H_2O_2 at neutral pH. Chemosphere 75(2):212–219. https://doi.org/10.1016/j.chemosphere.2008.12.002

Lee W, Batchelor B (2002) Abiotic reductive dechlorination of chlorinated ethylenes by iron-bearing soil minerals. 1. Pyrite and magnetite. Environ Sci Technol 36(23):5147–5154. https://doi.org/10.1021/es025836b

Lin Y, Yang C, Xiu R, Wang J, Wei Y, Sun Y (2014) Decolorization of methyl orange by green rusts with hydrogen peroxide at neutral pH. Water Sci Technol 69(2):371–377. https://doi.org/10.2166/wst.2013.716

Liu HZ, Bruton TA, Doyle FM, Sedlak DL (2014) In situ chemical oxidation of contaminated groundwater by persulfate: decomposition by Fe(III)- and Mn(IV)-containing oxides and aquifer materials. Environ Sci Technol 48(17):10330–10336. https://doi.org/10.1021/es502056d

Luo S, Wei Z, Dionysiou DD, Spinney R, Hu W-P, Chai L, Yang Z, Ye T, Xiao R (2017) Mechanistic insight into reactivity of sulfate radical with aromatic contaminants through single-electron transfer pathway. Chem Eng J 327:1056–1065. https://doi.org/10.1016/j.cej.2017.06.179

Luo S, Wei Z, Spinney R, Villamena FA, Dionysiou DD, Chen D, Tang C-J, Chai L, Xiao R (2018) Quantitative structure–activity relationships for reactivities of sulfate and hydroxyl radicals with aromatic contaminants through single–electron transfer pathway. J Hazard Mater 344:1165–1173. https://doi.org/10.1016/j.jhazmat.2017.09.024

Matta R, Hanna K, Chiron S (2008) Oxidation of phenol by green rust and hydrogen peroxide at neutral pH. Sep Purif Technol 61(3):442–446. https://doi.org/10.1016/j.seppur.2007.12.005

Mitsunobu S, Takahashi Y, Sakai Y (2008) Abiotic reduction of antimony(V) by green rust $(Fe_4(II)Fe_2(III)(OH)_{12}SO_4 \cdot 3H_2O$. Chemosphere 70(5):942–947. https://doi.org/10.1016/j.chemosphere.2007.07.021

Neta P, Huie RE, Ross AB (1988) Rate constants for reactions of inorganic radicals in aqueous-solution. J Phys Chem Ref Data 17(3):1027–1284. https://doi.org/10.1063/1.555808

O'Loughlin EJ, Larese-Casanova P, Scherer M, Cook R (2007) Green rust formation from the bioreduction of gamma-FeOOH (lepidocrocite): comparison of several Shewanella species. Geomicrobiol J 24(3–4):211–230. https://doi.org/10.1080/01490450701459333

Simon L, Francois M, Refait P, Renaudin G, Lelaurain M, Genin JMR (2003) Structure of the Fe(II-III) layered double hydroxysulphate green rust two from Rietveld analysis. Solid State Sci 5(2):327–334

Wander MCF, Rosso KM, Schoonen MAA (2007) Structure and charge hopping dynamics in green rust. J Phys Chem C 111(30):11414–11423. https://doi.org/10.1021/jp072762n

Wang D, Gilliland SE, Yi X, Logan K, Heitger DR, Lucas HR, Wang W-N (2018a) Iron mesh-based metal organic framework filter for efficient arsenic removal. Environ Sci Technol 52(7):4275–4284. https://doi.org/10.1021/acs.est.7b06212

Wang D, Pillai SC, Ho S-H, Zeng J, Li Y, Dionysiou DD (2018b) Plasmonic-based nanomaterials for environmental remediation. Appl Catal B 237:721–741. https://doi.org/10.1016/j.apcatb.2018.05.094

Yin WZ, Huang LZ, Pedersen EB, Frandsen C, Hansen HCB (2017) Glycine buffered synthesis of layered iron(II)-iron(III) hydroxides (green rusts). J Colloid Interface Sci 497:429–438. https://doi.org/10.1016/j.jcis.2016.11.076

Yu YT, Li SQ, Peng XZ, Yang SJ, Zhu YF, Chen L, Wu F, Mailhot G (2016) Efficient oxidation of bisphenol A with oxysulfur radicals generated by iron-catalyzed autoxidation of sulfite at circumneutral pH under UV irradiation. Environ Chem Lett 14(4):527–532. https://doi.org/10.1007/s10311-016-0573-3

Zhang XB, Ding ZX, Yang J, Cizmas L, Lichtfouse E, Sharma VK (2018) Efficient microwave degradation of humic acids in water using persulfate and activated carbon. Environ Chem Lett 16(3):1069–1075. https://doi.org/10.1007/s10311-018-0721-z

Zhou L, Sleiman M, Ferronato C, Chovelon JM, Richard C (2017) Reactivity of sulfate radicals with natural organic matters. Environ Chem Lett 15(4):733–737. https://doi.org/10.1007/s10311-017-0646-y